

Temperature Dependence of the Chemical Potential in Na_xCoO_2 : Implications for the Large Thermoelectric Power

Yukiaki Ishida¹, Hiromichi Ohta^{2,3}, Atsushi Fujimori¹, Hideo Hosono^{3,4}

¹*Department of Physics and Department of Complexity Science and Engineering,
University of Tokyo, Kashiwa, Chiba 277-8561, Japan,*

²*Graduate School of Engineering, Nagoya University, Furo-cho, Chikusa, Nagoya 464-8603, Japan,
3ERATO-SORST, JST, in Frontier Collaborative Research Center,*

*S2-6F East, Mail-box S2-13, Tokyo Institute of Technology,
4259 Nagatsuta-cho, Midori-ku, Yokohama 226-8503, Japan and*

*4Frontier Collaborative Research Center, S2-6F East, Mail-box S2-13,
Tokyo Institute of Technology, 4259 Nagatsuta-cho, Midori-ku, Yokohama 226-8503, Japan*

(Dated: December 2, 2024)

We have performed a temperature-dependent photoemission study of a Na_xCoO_2 ($x \sim 0.8$) epitaxial thin film prepared by the reactive solid-phase epitaxy method. The chemical potential shift as a function of temperature was derived from the Co 3d peak shift, and revealed a crossover from the degenerate Fermion state at low temperatures to the correlated hopping state of $\text{Co}^{3+}/\text{Co}^{4+}$ mixed-valence at high temperatures. This suggests that the large thermoelectric power at high temperatures should be considered in the correlated hopping picture.

PACS numbers: 72.15.Jf, 71.28.+d, 79.60.-i

Thermoelectric (TE) materials directly convert heat into electricity. Extensive effort has been made on search for efficient TE materials for practical applications such as Peltier refrigerators and TE batteries [1, 2, 3]. While heavily doped semiconductors have been considered as promising TE materials, the recent report on the large TE power in Na_xCoO_2 ($x > 0.5$, $\sim 100 \mu\text{V/K}$ at room temperature) attracted much interest because it also showed metallic and hence high conductivity [4]. In conventional metals, one expects small TE power caused by metallic diffusion typically of several $\mu\text{V/K}$ arising from the energy dependence of the conductivity around the electron chemical potential μ [1, 5]. Thermodynamic properties of metallic Na_xCoO_2 ($x > 0.5$) are also anomalous: it exhibits a large electronic specific-heat coefficient [6] and a Curie-Weiss magnetic susceptibility [7], which can be attributed to strong electron correlation [8]. Therefore, it should be clarified whether the origin of the large TE power involves strong electron correlation effects or not. Based on the strong correlation limit, Koshiba, Tsutsui and Maekawa [9] explained the large TE using a Heikes formula to include the spin-orbital degeneracies of the Co^{3+} and Co^{4+} ions. On the other hand, the largeness of the TE was discussed within the Boltzmann transport theory [10, 11].

By photoemission spectroscopy (PES), one measures the single-particle spectral function whose energy abscissa is referenced to μ . Therefore, PES is a powerful tool not only to investigate the quasi-particle (QP) dynamics of materials but also the thermodynamic quantities like μ [12, 13, 14]. Previous PES studies on bulk Na_xCoO_2 ($x > 0.5$) have revealed a QP peak developing in the narrow energy region within $\sim 100 \text{ meV}$ from μ [15, 16, 17]. The derived hopping amplitude t of the Co 3d electrons was extremely small ($|t| \sim 10 \text{ meV}$ [16, 17]) compared to band-structure calculation ($|t| \sim 130 \text{ meV}$ [10]), indicating

strong correlation effect. Interestingly, the QP peak disappeared above $\sim 200 \text{ K}$ [15, 17], where the TE becomes large. Beyond the $\sim 100 \text{ meV}$ region, the spectrum becomes broadened and dispersionless, and a Gaussian-like peak typical of low-spin t_{2g} electron systems is observed [16, 18]. This is in strong contrast to the band-structure calculations [10], where dispersions with typical bandwidths of $\sim 1 \text{ eV}$ extend over the entire valence-band region. This discrepancy between band theory and PES spectra is reminiscent of the underdoped cuprates [19] and the colossal magnetoresistive manganites [20], where spectral weight near μ is vanishingly small compared to strong incoherent structures residing at higher binding energies.

In this Letter, we report on the temperature dependence of the Co 3d-derived single-particle spectral function including the incoherent part, to obtain information about the electronic structure responsible for the large TE power. Here, we have made temperature-dependent PES measurements on a single crystalline epitaxial thin film of Na_xCoO_2 ($x = 0.83$) [21]. Epitaxial thin film surfaces are, in general, stable compared to the fractured surfaces of bulk single crystals, and thus advantageous for surface sensitive PES measurements particularly for temperature cycling [22].

A $\text{Na}_{0.83}\text{CoO}_2$ epitaxial thin film of $\sim 1500 \text{ \AA}$ thickness was prepared by the reactive solid-phase epitaxy (R-SPE) method. Details of the R-SPE method are described elsewhere [21]. After the final step of the R-SPE method, namely, after having annealed the sample with a yttria-stabilized-zirconia (YSZ) coverplate with NaHCO_3 powder in an electric furnace, the sample was immediately transferred into the preparation chamber of the spectrometer. In order to recover the clean surface, the sample was again covered with the YSZ plate and annealed under the 1 atmO_2 (99.9999 %) atmosphere for 30 min

at 550°C using a Pt annealing system. After the surface treatment, the preparation chamber was quickly vented to $\sim 1.0 \times 10^{-7}$ Torr, the YSZ plate was dropped off, and the sample was transferred without exposure to air into the main chamber (base pressure $\sim 1 \times 10^{-10}$ Torr). The Al $K\alpha$ line ($h\nu=1486.6$ eV) and the monochromatized He I line ($h\nu=21.22$ eV) were used as excitation sources, and the photoelectrons were collected using a Scienta SES-100 analyzer. Typical energy resolution was 13 meV for He I and 0.8 eV for Al $K\alpha$.

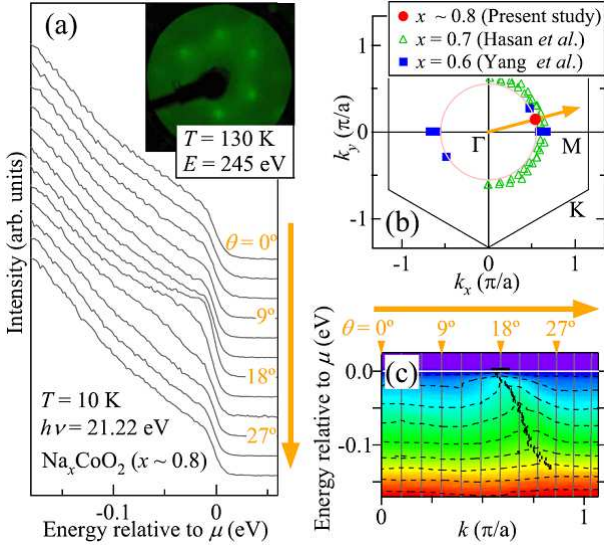


FIG. 1: (Color) ARPES spectra of Na_xCoO_2 thin film prepared using the R-SPE method. (a) Energy distribution curves. Inset: LEED pattern for electron beam energy of 245 eV. (b) Brillouin zone of the triangular lattice. Orange arrow indicates the direction of the recorded dispersion. k_F 's determined from the present study and those reported by Yang *et al.* [16] and Hasan *et al.* [17] are indicated. (c) Intensity plot in the E - k plane. Red/blue corresponds to high/low intensity. QP dispersion is traced by the black dots.

Figure 1(a) shows the angle-resolved PES (ARPES) spectra of the Na_xCoO_2 thin film. We observed a clear dispersion from the Γ point toward the Brillouin zone boundary along a cut indicated by an orange arrow in Fig. 1(b), as well as the six-fold LEED pattern shown in the inset of Fig. 1(a) reflecting the triangular lattice. These results indicate that a clean single crystalline surface was obtained after the R-SPE treatment. The QP dispersion crosses μ at $k_F \sim 0.56\frac{\pi}{a}$ (a : Co-Co distance) in the E - k plane [Fig. 1(b)]. From comparison with the previous studies [16, 17], the present Fermi-surface volume is in the range of $x \gtrsim 0.6$ [Fig. 1(b)], in agreement with the value $x=0.83$ determined from the lattice constant [21]. This indicates that the Na evaporation during the oxygen annealing was successfully minimized even at the outermost layer of the thin film by using the YSZ coverplate. Hereafter, we consider the Na concentration of the measured Na_xCoO_2 surface to be $x \sim 0.8$.

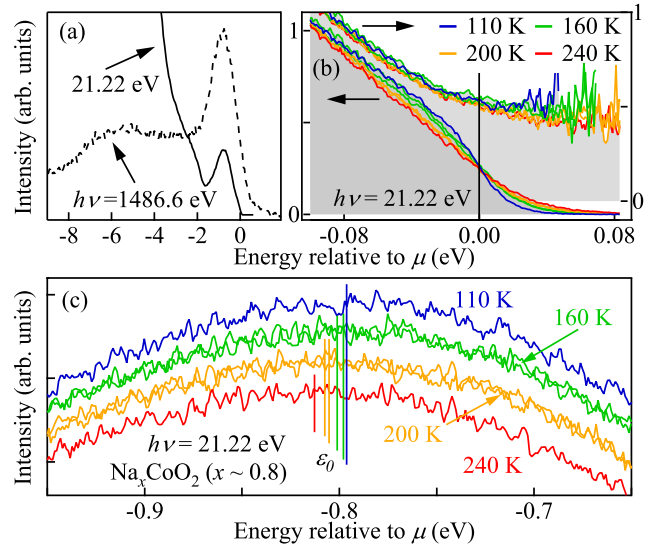


FIG. 2: (Color) Temperature dependence of the angle-integrated PES spectra of $\text{Na}_{\sim 0.8}\text{CoO}_2$. (a) Valence-band spectra using photon energies of 21.22 eV and 1486.6 eV. (b) Temperature dependence of PES spectra in the region near μ (left axis). The temperature was cycled as 160→110→160→200→240→200 (in units of K). The spectra devided by the Fermi-Dirac function are also plotted (right axis). (c) Temperature dependence in the Co 3d t_{2g} peak region. Spectra have been offset according to the measuring temperature. The peak positions are indicated by vertical bars.

Next, we studied temperature dependence of the Co 3d-derived peak which is centered at ~ 0.8 eV below μ as shown in Fig. 2. Here we note that the ~ 0.8 eV peak was observed even when we increased the bulk sensitivity of PES using the higher excitation energy of 1486.6 eV, as shown in Fig. 2(a). This suggests that the broad ~ 0.8 eV peak and the smallness of the QP spectral weight near μ are intrinsic bulk electronic properties. The spectra at various temperatures near μ are plotted in Fig. 2(b) (left axis). We have also plotted the spectra devided by the Fermi-Dirac function so as to obtain the information about the DOS around μ . At low temperatures, one can see a clear Fermi cut-off, reflecting the metallic character of Na_xCoO_2 [4], and a negative slope in the DOS around μ , which, within the degenerate-Fermion model, can cause an upward shift of μ with temperature (described later). The spectra show that the temperature dependence near μ is largely due to that of the Fermi-Dirac function. On the other hand, as shown in Fig. 2(c), the enlarged plot around 0.8 eV shows that the Co 3d t_{2g} peak is shifted to higher binding energies with temperature, which occurred reproducibly during the temperature cycling. A similar tendency was observed in the ARPES study of Ref. [17]. Here, the Co 3d t_{2g} peak positions (ε_0) have been determined by fitting the region $\sim -0.8 \pm 0.1$ eV to Gaussians, and are indicated by vertical bars.

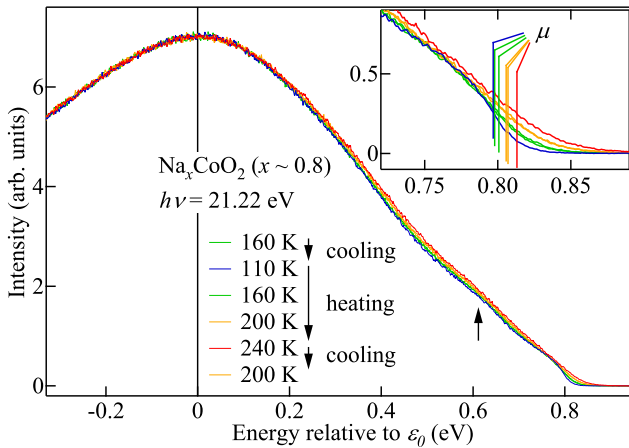


FIG. 3: (Color) Temperature dependence of the Co 3d t_{2g} peak and chemical potential shift. The spectra have been aligned at the peak position ε_0 and normalized to the height of the peak. An arrow at ~ 0.6 eV above ε_0 indicate the hump structure. Inset: enlarged view near μ . The energy positions of μ 's are indicated by vertical bars.

Figure 3 shows the temperature dependence of the PES spectra of the entire Co 3d t_{2g} peak region with the peak position ε_0 aligned. One can see that the Co 3d t_{2g} peak was broadened with increasing temperature. One may also notice a hump-like structure indicated by an arrow in Fig. 3 at ~ 0.2 eV below μ , which was assigned to the e'_g states in Ref. [23]. We note that this hump also showed a temperature broadening. A similar temperature broadening of the peak in PES has been observed in the core-level PES studies on ionic crystals [24, 25], and in the lower Hubbard bands of the insulating phase of VO_2 [22, 26], $\text{Sr}_2\text{CuO}_2\text{Cl}_2$ [27], and $\text{Ca}_2\text{CuO}_2\text{Cl}_2$ [27, 28]. The broadening has been analyzed with the model where the localized photohole is coupled to a boson mode such as local lattice vibrations [14, 22, 24, 25, 28, 29]. Therefore, we could similarly attribute the temperature broadening of the Co 3d peak as the effect of localized Co 3d photohole coupled to a boson mode such as local lattice vibrations. The coherent QP peak shown in Fig. 1(a) can then be understood as developing from the zero-boson line, whose spectral weight is small. Since the centroid of the peak is independent of T within the the electron-boson coupling model discussed above [29], the position of the incoherent structure ε_0 serves as the energy reference for μ . Therefore, we interpret the peak shift shown in Fig. 2(c) as due to the shift of μ , as shown in the inset of Fig. 3(a). The chemical potential shift $\Delta\mu$ thus deduced is plotted in Fig. 4 as a function of T . We have also plotted $\Delta\mu$ derived from the temperature dependent PES measurements performed in the cooling series below $T=150$ K.

In conventional metals in which charge carriers are degenerate Fermions, finite $\frac{\partial\mu}{\partial T}$ arises from the finite slope in the DOS around μ . $\Delta\mu$ is estimated within this model

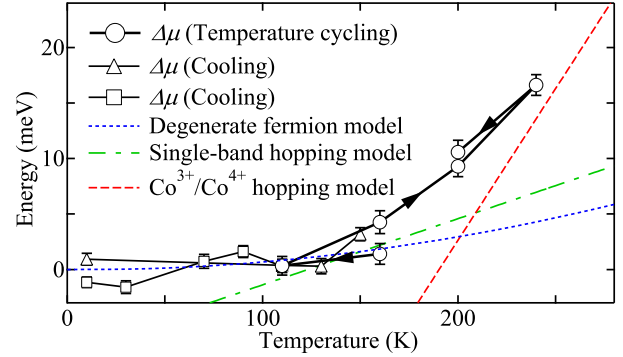


FIG. 4: (Color) Chemical potential shift $\Delta\mu$ of Na_xCoO_2 ($x \sim 0.8$) derived from the PES spectra. $\Delta\mu$ estimated from the degenerate Fermion model and the slopes of $\Delta\mu$'s for the single-band hopping [30] and correlated-hopping model of low-spin $\text{Co}^{3+}/\text{Co}^{4+}$ mixed-valence state [9] are plotted for comparison (see, text). The error bars for $\Delta\mu$ are $\pm\sigma$ of the Co 3d peak fitting.

using the DOS in the inset of Fig. 2(a) and plotted in Fig. 4 (dotted line). One immediately notice that the observed $\Delta\mu$ strongly deviates from the degenerate Fermion model above ~ 200 K. This temperature coincides with the temperature above which the QP peak disappears in the ARPES spectra [15, 17]. The results may be interpreted as follows: Above the characteristic temperature $T^* \sim 200$ K, the broadning of the Fermi-Dirac function $\sim 4k_B T$ exceeds the width of the narrow QP band ~ 100 meV [16, 17]. Then, the QP's can no more be described as degenerate Fermions and behave as classical particles undergoing thermally activated correlated hopping among the Co sites. For such carriers, the configurational entropy density s and hence $\frac{\partial\mu}{\partial T} = -\frac{\partial s}{\partial x}$, where x is the number of electron carriers per site, can be calculated following Ref. [30]. In the case of $\text{Co}^{3+}/\text{Co}^{4+}$ mixed-valence state [9],

$$\frac{\partial\mu}{\partial T} = -k_B \ln\left(\frac{g_3}{g_4} \frac{1-x}{x}\right), \quad (1)$$

where g_3 and g_4 are the spin-orbital degeneracies of Co^{3+} and Co^{4+} , respectively, and x is the fraction of Co^{3+} ions. Here, we note that the presence of electron-boson coupling discussed above does not affect eq. (1). In Fig. 4, we have plotted $\Delta\mu = -k_B \ln\left(\frac{g_3}{g_4} \frac{1-x}{x}\right) \times T + \text{const.}$ for $g_3=1$, $g_4=6$, and $x=0.8$, corresponding to the low-spin $\text{Co}^{3+}/\text{Co}^{4+}$ mixed-valence state with a dashed line [9], and that for $g_3=1$, $g_4=2$, and $x=0.8$ with a dot-dashed line, which corresponds to the single-band hopping model [30]. One can recognize that the experimentally derived $\Delta\mu$ crossovers at T^* from the degenerate Fermion model to the localized-electron model as the temperature is increased.

The above result for $\Delta\mu$ suggests that the transport properties should also be treated within the correlated hopping model in the high temperature regime $T > T^*$

[30]. First of all, the largeness of the TE power has indeed been attributed to the large spin-orbital entropy of low-spin $\text{Co}^{3+}/\text{Co}^{4+}$ mixed-valence state, since, at high enough temperatures, the TE power (Seebeck coefficient) is dominated by the entropy term $\frac{k}{T}$ compared to the energy-transport term associated with the kinetic energies of carriers [9, 30, 31]. The high temperature Hall coefficient also shows anomalous increase with T [32, 33], and its origin was discussed in terms of the hopping effect on the triangular lattice of $\text{Co}^{3+}/\text{Co}^{4+}$ [33]. On the other hand, the suppressed $\Delta\mu$ at the low temperature regime $T < T^*$ indicate that the carriers are degenerate, and hence Boltzmann type transport for degenerate Fermion model may become valid [10, 11]. Nevertheless, the novel magnetic-field suppression of the TE power is observed already at $T=2.5$ K [34]. DC resistivity indicates anomalously large electron-electron scattering rate at $T < 1$ K, which is also suppressed in a magnetic field [35]. These observations indicate that the degenerate Fermion excitations below T^* has another low energy/temperature scale ($\ll 200$ K) influenced by strong correlation.

In conclusion, the experimentally derived chemical potential shift as a function of temperature in Na_xCoO_2 revealed a crossover from the low-temperature degenerate Fermion state to the high-temperature correlated hopping state involving the spin-orbital degeneracy of the $\text{Co}^{3+}/\text{Co}^{4+}$ mixed-valence at a characteristic temperature $T^* \sim 200$ K. The anomalous transport properties at high temperatures such as the large TE power and the unsaturated Hall coefficient with temperatures should thus be treated within the correlated hopping model. The present work has demonstrated that the temperature-dependent chemical potential shift can be used as a measure of correlation effects in orbitally degenerate systems.

We thank K. Sugiura for collaboration, T. Mizokawa, K.M. Shen and K. Okazaki for discussion, K. Tanaka, H. Yagi, H. Wadati, M. Hashimoto, M. Takizawa and M. Kobayashi for help in experiment. This work was supported by a Grant-in-Aid for Scientific Research in Priority Area (16204024) from the Ministry of Education, Culture, Sports, Science and Technology, Japan.

[1] G. Mahan, B. Sales, and J. Sharp, Phys. Today **50** No. 3, 42 (1997).

[2] F.J. DiSalvo, Science **285**, 703 (1999).

[3] B.C. Sales, Science **295** 1248 (2002).

[4] I. Terasaki, Y. Sasago, and K. Uchinokura, Phys. Rev. B **56**, R12685 (1997).

[5] R.D. Barnard, *Thermoelectricity in metals and alloys* (Taylor & Francis, London, 1972).

[6] Y. Ando, N. Miyamoto, K. Segawa, T. Kawata, and I. Terasaki, Phys. Rev. B **60**, 10580 (1999).

[7] R. Ray, A. Ghoshray, K. Ghoshray, and S. Nakamura, Phys. Rev. B **59**, 9454 (1999).

[8] M. Imada, A. Fujimori, and Y. Tokura, Rev. Mod. Phys. **70**, 1039 (1998).

[9] W. Koshibae, K. Tsutsui, and S. Maekawa, Phys. Rev. B **62**, 6869 (2000).

[10] D.J. Singh, Phys. Rev. B **61**, 13397 (2000).

[11] T. Takeuchi, T. Kondo, T. Takami, H. Takahashi, H. Ikuta, U. Mizutani, K. Soda, R. Funahashi, M. Shikano, M. Mikami, S. Tsuda, T. Yokoya, S. Shin, and T. Muro, Phys. Rev. B **69**, 125410 (2004).

[12] A. Ino, T. Mizokawa, A. Fujimori, K. Tamasaku, H. Eisaki, S. Uchida, T. Kimura, T. Sasagawa, and K. Kishio, Phys. Rev. Lett. **79**, 2101 (1997).

[13] A. Fujimori, A. Ino, J. Matsuno, T. Yoshida, K. Tanaka, and T. Mizokawa, J. Electron Spectrosc. Relat. Phenom. **124**, 127 (2002).

[14] K.M. Shen, F. Ronning, D.H. Lu, W.S. Lee, N.J.C. Ingle, W. Meevasana, F. Baumberger, A. Damascelli, N.P. Armitage, L.L. Miller, Y. Kohsaka, M. Azuma, M. Takano, H. Takagi, and Z.-X. Shen, Phys. Rev. Lett. **93**, 267002 (2004).

[15] T. Valla, P.D. Johnson, Z. Yusof, B. Wells, Q. Li, S.M. Loureiro, R.J. Cava, M. Mikami, Y. Mori, M. Yoshimura, and T. Sasaki, Nature (London) **417**, 627 (2002).

[16] H.-B. Yang, S.-C. Wang, A.K.P. Sekharan, H. Matsui, S. Souma, T. Sato, T. Takahashi, T. Takeuchi, J.C. Campuzano, R. Jin, B.C. Sales, D. Mandrus, Z. Wang, and H. Ding, Phys. Rev. Lett. **92**, 246403 (2004).

[17] M.Z. Hasan, Y.-D. Chuang, D. Qian, Y.W. Li, Y. Kong, A.P. Kuprin, A.V. Fedorov, R. Kimmerling, E. Rotenberg, K. Rossnagel, Z. Hussain, H. Koh, N.S. Rogado, M.L. Foo, and R.J. Cava, Phys. Rev. Lett. **92**, 246402 (2004).

[18] T. Mizokawa, L.H. Tjeng, P.G. Steeneken, N.B. Brookes, I. Tsukada, T. Yamamoto, and K. Uchinokura, Phys. Rev. B **64**, 115104 (2001).

[19] A. Damascelli, Z. Hussain, and Z.-X. Shen, Rev. Mod. Phys. **75**, 473 (2003).

[20] D.S. Dessau, T. Saitoh, C.-H. Park, Z.-X. Shen, P. Villella, N. Hamada, Y. Moritomo, and Y. Tokura, Phys. Rev. Lett. **81**, 192 (1998).

[21] H. Ohta, S-W. Kim, S. Ohta, K. Koumoto, M. Hirano, and H. Hosono, Cryst. Growth Des. **5**, 25 (2005).

[22] K. Okazaki, A. Fujimori, T. Yamauchi, and Y. Ueda, Phys. Rev. B **69**, 140506(R) (2004).

[23] H.-B. Yang, Z.-H. Pan, A.K.P. Sekharan, T. Sato, S. Souma, T. Takahashi, R. Jin, B.C. Sales, D. Mandrus, A.V. Fedorov, Z. Wang, and H. Ding, Phys. Rev. Lett. **95**, 146401 (2005).

[24] P.H. Citrin, P. Eisenberger, and D.R. Hamann Phys. Rev. Lett. **33**, 965 (1974).

[25] M. Iwan and C. Kunz, Phys. Lett. **60A**, 345 (1977).

[26] K. Okazaki, A. Fujimori, and M. Onoda, J. Phys. Soc. Jpn. **71**, 822 (2002).

[27] C. Kim, F. Ronning, A. Damascelli, D.L. Feng, Z.-X. Shen, B.O. Wells, Y.J. Kim, R.J. Birgeneau, M.A. Kastner, L.L. Miller, H. Eisaki, and S. Uchida, Phys. Rev. B **65**, 174516 (2002).

- [28] K.M. Shen, F. Ronning, W. Meevasana, D.H. Lu, N.J.C. Ingle, F. Baumberger, W.S. Lee, L.L. Miller, Y. Kohsaka, M. Azuma, M. Takano, H. Takagi, and Z.-X. Shen, (unpublished).
- [29] G.D. Mahan, *Many-Particle Physics* (Plenum, New York, 1981).
- [30] P.M. Chaikin and G. Beni, Phys. Rev. B **13**, 647 (1976).
- [31] W. Koshibae and S. Maekawa, Phys. Rev. Lett. **87**, 236603 (2001).
- [32] M.L. Foo, Y. Wang, S. Watauchi, H.W. Zandbergen, T. He, R.J. Cava, and N.P. Ong, Phys. Rev. Lett. **92**, 247001 (2004).
- [33] Y. Wang, N.S. Rogado, R.J. Cava, and N.P. Ong, cond-mat/035455.
- [34] Y. Wang, N.S. Rogado, R.J. Cava, and N.P. Ong, Nature (London) **423**, 425 (2003).
- [35] S.Y. Li, L. Taillefer, D.G. Hawthorn, M.A. Tanatar, J. Paglione, M. Sutherland, R.W. Hill, C.H. Wang, and X.H. Chen, Phys. Rev. Lett. **93**, 056401 (2004).